

Anisotropic resistivity and paraconductivity of $\text{Tl}_2\text{Ba}_2\text{CaCu}_2\text{O}_8$ single crystals

H. M. Duan

Physics Department, University of Colorado, Boulder, Colorado 80309

W. Kiehl

Physics Department, University of Arkansas, Fayetteville, Arkansas 72701

C. Dong

Physics Department, University of Colorado, Boulder, Colorado 80309

A. W. Cordes

Chemistry Department, University of Arkansas, Fayetteville, Arkansas 72701

M. J. Saeed and D. L. Viar

Physics Department, University of Arkansas, Fayetteville, Arkansas 72701

A. M. Hermann

Physics Department, University of Colorado, Boulder, Colorado 80309

(Received 21 June 1990; revised manuscript received 13 February 1991)

The anisotropic resistivity and paraconductivity of $\text{Tl}_2\text{Ba}_2\text{CaCu}_2\text{O}_8$ single crystals were measured. The in-plane and c -axis resistivities are, respectively, $\sim 7 \times 10^{-4}$ and 10^{-1} Ω cm at room temperature. The c -axis resistivity decreases with decreasing temperature in the temperature range from room temperature down to the superconducting transition temperature, and the second derivative of ρ_c is negative, which is not characteristic of $\text{YBa}_2\text{Cu}_3\text{O}_7$ and $\text{Bi}_2\text{Sr}_{2.2}\text{Ca}_{0.8}\text{Cu}_2\text{O}_8$ single crystals, in which the second derivative is either positive or zero. The in-plane paraconductivity is obtained from the in-plane resistivity, and a method without the critical temperature as an adjustable parameter is employed to obtain the dimensionality. The data show that the superconductivity is two dimensional, but a crossover from two to three dimensions has also been observed near the transition temperature in some samples.

INTRODUCTION

Since the discovery of high-temperature superconductivity in the doped copper-oxide systems, there has been much interest in the usual properties of these systems in their normal state. The highly anisotropic electronic structure of the carrier planes and the interaction between the planes are very interesting aspects of the nature of these systems. In the normal state, the resistivity ratio ρ_c/ρ_p (where ρ_c and ρ_p are the resistivities along the c axis and in the a - b planes, respectively) was reported to be as high as 10^2 – 10^5 , and thermal excitation transport in the normal state was observed in the c axis of $\text{YBa}_2\text{Cu}_3\text{O}_7$ and $\text{Bi}_2\text{Sr}_{2.2}\text{Ca}_{0.8}\text{Cu}_2\text{O}_8$ crystals.^{1–5} The dimensionality of the superconductivity has been discussed in relation to paraconductivity measurements on bulk, thin-film, and single-crystal samples of $\text{YBa}_2\text{Cu}_3\text{O}_7$ (Refs. 6–8) and $\text{Bi}_2\text{Sr}_{2.2}\text{Ca}_{0.8}\text{Cu}_2\text{O}_8$.⁹ In the Tl - Ba - Ca - Cu - O system, measurements were carried out on polycrystalline thin-film and bulk samples.^{9,10}

In this paper, we report the results of anisotropic resistivity and paraconductivity measurements on single crystals of $\text{Tl}_2\text{Ba}_2\text{CaCu}_2\text{O}_8$ (2:2:1:2). The ρ_p versus T behavior shows an increase with increasing temperature and is approximately linear above 220 K. Below 220 K, the

curve gradually deviates from the linear behavior. In our experiments, ρ_c decreases as the temperature decreases, and the ρ_c versus T curve is not linear, the second derivative is negative. The ρ_c - T curve saturates as temperature increases, this may be explained by a resistivity model of a metallic system where the mean free path is close to the Mott limit. We believe the electronic band structure of 2:2:1:2 corresponds to that of a three-dimensional metal with a large anisotropic effective mass. In some crystals, paraconductivity may be fit by a two-dimensional theory in the temperature range from 150 to ~ 2 K above transition temperature (~ 102 K), but in other samples, a crossover from two- or three-dimensional behavior occurs at ~ 5.5 K above the transition temperature.

EXPERIMENT

Two different processes were used to grow the single crystals. In the first process (A), we used a $\text{Ba}_2\text{Ca}_2\text{Cu}_3\text{O}_x$ precursor. Appropriate amounts of BaO , CaO , and CuO (each 99.99% pure) were mixed and ground to form a mixture with a nominal stoichiometry of $\text{Ba}_2\text{Ca}_2\text{Cu}_3\text{O}_x$. The mixture was heated in air for 24 h at 920°C, with an intermediate grinding carried out in order to facilitate a complete reaction. The reacted mixture was then ground

again to form the precursor powder. Proper amounts of precursor and Ti_2O_3 powders were mixed and ground to form a powder with a nominal stoichiometry of $\text{Ti}_2\text{Ba}_2\text{Ca}_2\text{Cu}_3\text{O}_x$. This powder was then pressed in pellet form under a pressure of 460 kg/cm^2 (6500 lb/in^2). Pellets of mass 25 g were placed in an Al_2O_3 crucible which was then loosely covered by an Al_2O_3 plate to protect the Ti_2O_3 from direct evaporation. The crucible was then put into a quartz tube which was located in a horizontal tube furnace. Because the mixture melted at $\sim 938^\circ\text{C}$, a 15-min heating period at $940\text{--}945^\circ\text{C}$ melted most of the mixture. The melt was then cooled to 900°C at a rate of 0.2°C/min . When it was cooled, crystals were formed. The nucleation was followed by a 1°C/min cooling to 700°C , 2°C/min to 400°C and 5 or more hours of furnace cooling to room temperature. This procedure was designed to relieve some inner stress and optimize the oxygen distribution and crystal structure. The entire process of heating the pellet occurred in flowing oxygen. In the second process (B), the precursor preparation step was skipped. Appropriate amounts of Ti_2O_3 , BaO , CaO , and CuO were ground to form a powder with a nominal composition of $\text{Ti}_2\text{Ba}_2\text{Ca}_2\text{Cu}_3\text{O}_x$. The remaining procedures were the same as in process A.

Like other Cu-O-based high- T_c superconducting single crystals, the crystals were rectangular plates with typical dimensions of $2 \text{ mm} \times 2 \text{ mm} \times 0.2 \text{ mm}$. X-ray dot maps and x-ray photoemission spectroscopy (XPS) results show the crystals were chemically uniform with stoichiometries of $\text{Ti}_2\text{Ba}_2\text{CaCu}_2\text{O}_8$ and $\text{Ti}_2\text{Ba}_2\text{Ca}_2\text{Cu}_3\text{O}_{10}$ (2:2:2:3). The x-ray four-circle diffraction verified that the 2:2:1:2 single crystals had high quality and no minor misoriented phase could be found. However, in the 2:2:2:3 phase grains, which we also have grown, sometimes two or three subgrains were observed with a few degrees of misorientation. X-ray diffraction confirmed the c axis was perpen-

dicular to the large rectangular dimensions. We present results of measurements of 2:2:1:2 crystals in this report.

The standard Montgomery method¹¹ was employed to measure the anisotropic resistivities. Contacts, with resistance less than 2Ω , were made by pure indium or other low-melting-point indium alloys such as Ag-In, Sn-In, or Pb-Sn-In. The contacts were located on the corners of the a - b planes. Since the alloy pads were less than $50 \mu\text{m}$ in diameter (less than one-tenth of the size of the smallest sample in these experiments), the deviation from the ideal condition was negligible.¹² Platinum fibers, $20 \mu\text{m}$ in diameter, was used to electrically connect the metallic pads to copper leads. A lock-in amplifier measured the voltage on two contacts when a $500 \mu\text{A}$ rms current at 87 Hz passed through the other two contacts (see top left of Fig. 1). Samples were Ohmic up to 10 mA . A thermometer with 0.2-K accuracy was used to measure the temperature; the temperature ramp rate was kept to 1 K/min . The resistance versus temperature curves were repeatable with thermal cycling to within 1% . The homogeneity of the crystals has also been confirmed by SQUID magnetometry measurements, in which only one sharp single transition was observed at 105 K .¹³

RESULTS AND DISCUSSION

The inset of Fig. 1 shows the typical temperature dependence of the Montgomery resistances. The R_c (R_p) represents the ratio of the voltage cross the contacts A, B (D, B) and the excitation current through C, D (A, C). In comparison to the $\text{YBa}_2\text{Cu}_3\text{O}_7$ and $\text{Bi}_2\text{Sr}_{2.2}\text{Ca}_{0.8}\text{Cu}_2\text{O}_8$ systems,^{1,2} the ratio R_c/R_p of the 2:2:1:2 single crystals changes with temperature less in the temperature range studied, especially near transition point, where the ratio in $\text{YBa}_2\text{Cu}_3\text{O}_7$ and $\text{Bi}_2\text{Sr}_{2.2}\text{Ca}_{0.8}\text{Cu}_2\text{O}_8$ changes rapidly. The resistance compounds R_p and R_c may be transformed into the resistivity components ρ_c and ρ_b by using an equivalent rectangle which maps the internal electric field. The resistivity components are shown in Fig. 1. In more than 10 samples studied, the room-temperature in-plane resistivities ranged from 6.5 to $8.5 \times 10^{-4} \Omega \text{ cm}$, while the c -axis room-temperature resistivity had a relative higher spread from 0.1 to $0.4 \Omega \text{ cm}$. Similar behavior was observed in the thermoelectric-power (TEP) measurements.¹⁴ A wider spread ($\Delta S/S \sim 25\%$, $T=300 \text{ K}$) was observed along the c axis, while in-plane TEP data from different crystals were in good agreement ($\Delta S/S < 3\%$, $T=300 \text{ K}$).¹⁴

An interesting feature of the electronic properties of high- T_c superconductors is the temperature dependence of the c -axis normal-state resistivity. In $\text{YBa}_2\text{Cu}_3\text{O}_7$ and $\text{Bi}_2\text{Sr}_{2.2}\text{Ca}_{0.8}\text{Cu}_2\text{O}_8$ crystals, both positive and negative slopes in the ρ versus T curves were observed (the positive sign was in the high-temperature region), but the second derivative was either positive or zero in all the data reported.¹⁻⁵ In $\text{YBa}_2\text{Cu}_3\text{O}_7$, Hagen *et al.* fit the ρ_c versus T curve with the formula $AT + B/T$,² with the term linear in T proposed as due to contact misalignment. The positive curvature is from the $1/T$ term which Anderson and co-workers have explained as the excitation transport tunneling between charge carrier planes.¹⁵

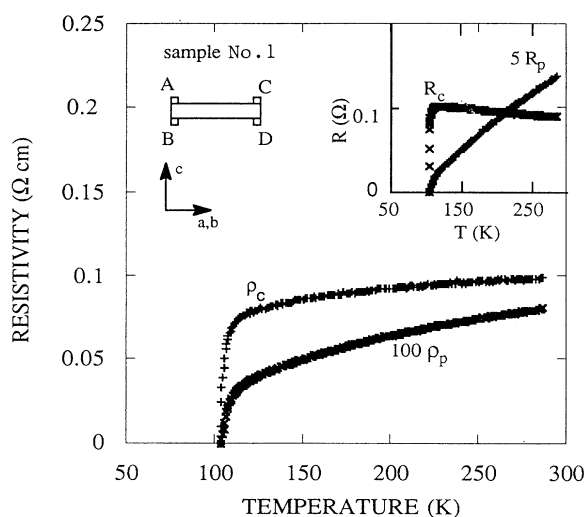


FIG. 1. Temperature dependence of resistivities. ρ_p is multiplied by 100. The inset shows the measured resistances by using the top left configuration (see text).

In $\text{Bi}_2\text{Sr}_{2.2}\text{Ca}_{0.8}\text{Cu}_2\text{O}_8$ crystals, a model of a thermally activated c -axis defect topology array, which is electrically linked together by the a - b plane forming a pass-through in the c direction, was proposed to explain the positive derivative at high temperature and negative derivative at low temperatures.³ The positive second derivative can be explained by thermal excitation transport.³ In the above models, the electronic bands are not metallic along the c axis. The positive second derivative of the activation term in these two models proposed for $\text{YBa}_2\text{Cu}_3\text{O}_7$ and $\text{Bi}_2\text{Sr}_{2.2}\text{Ca}_{0.8}\text{Cu}_2\text{O}_8$ would not agree with our 2:2:1:2 experimental results, which show a negative second derivative in the entire temperature range investigated.

We notice that the ρ_c - T curves are similar to the resistivity of some organic conductors. Different attempts to fit a T^n temperature dependence, which the organic superconductors usually follow, failed. The ρ_c versus T curves change from a low slope at high temperature to a high slope at low temperature, which is similar to the saturation tendencies in the conventional $A15$ superconductors V_3Si and Nb_3Sn (Refs. 16 and 17) (although the resistivity values reported here are about 3 orders of magnitude higher).

We suggest that the coexistence of the saturation of ρ_c and the linearity of ρ_p in the same temperature region is due to the anisotropic crystal and electronic band structure. For the electrons in a conduction band, the mean free path $l = v_F\tau$, where v_F is the Fermi velocity and τ is the relaxation time which is limited by the scattering of structure defects and phonons in the sample. Fermi velocity is proportional to the inverse of the effective mass m^* , $v_F \propto 1/m^*$, and therefore $l \propto 1/m^*$. Since the effective mass is highly anisotropic, $l_{\parallel} \gg l_{\perp}$. Furthermore, along the c axis, the distances between conduction planes, Cu-O planes, and possibly Tl-O planes, is about $\sim 5 \text{ \AA}$ which is \sim three times larger than the interatomic spacing in the conduction planes. The minimum scattering length for the c axis would be a few times larger than that in the a - b plane. The combination of a small mean free path and a larger minimum scattering length makes the c -axis resistivity saturate in a much lower-temperature region. Hence, ρ_c could be saturating, where the length of the mean free path approaches the Mott limit, meanwhile ρ_p is in a linear region where the length of the mean free path is far from the Mott limit. (The linear in-plane resistivities of $\text{YBa}_2\text{Cu}_3\text{O}_7$ and $\text{La}_{1.825}\text{Sr}_{0.175}\text{CuO}_4$ suggest that the mean free path is at least 5.5 and 7.6 times longer, respectively, than the Mott limit at room temperature.¹⁸)

It is unusual that the 2:2:1:2 resistivity along the c axis appears metallic with a resistivity of the order of $10^{-1} \Omega \text{ cm}$. The $A15$ metals V_3Si , Nb_3Sn , and Nb_3Sb , saturate at the resistivity of $150 \mu\Omega \text{ cm}$,^{16,17} which is even much smaller than the in-plane resistivities of high- T_c superconductors. We also notice reports of linearity of the ρ_c - T curve in $\text{YBa}_2\text{Cu}_3\text{O}_7$ when the magnitude of ρ_c is as high as $10^{-2} \Omega \text{ cm}$.^{4,5} Following the arguments in Ref. 18, we note that the length of mean free path in $\text{YBa}_2\text{Cu}_3\text{O}_7$ along the c direction could be almost an order of magnitude larger than the Mott limit. This im-

plies, in $\text{YBa}_2\text{Cu}_3\text{O}_7$, that the ρ_c - T curve may be metallic when the resistivity is as high as $10^{-1} \Omega \text{ cm}$, where the mean free path is few times the Mott limit. The structural similarity of the high- T_c systems suggests that the results of $\text{YBa}_2\text{Cu}_3\text{O}_7$ and 2:2:1:2 Tl-Ba-Ca-Cu-O should not be inconsistent and we see this consistency experimentally. Furthermore, we note the difference between the temperature dependence of the anisotropic TEP in the $\text{YBa}_2\text{Cu}_3\text{O}_7$ and 2:2:1:2 Tl-Ba-Ca-Cu-O single crystals.^{1,19,20} In $\text{YBa}_2\text{Cu}_3\text{O}_7$ the c -axis TEP, S_c , decreases monotonically from 300 K to T_c ($\sim 90 \text{ K}$), while the in-plane TEP, S_p , increases as temperature decreases. In our 2:2:1:2 crystals,¹⁴ as the temperature decreases, S_p increases (as is the case for $\text{YBa}_2\text{Cu}_3\text{O}_7$ single crystals), but in the c direction the TEP of the 2:2:1:2 crystals increases monotonically (in contrast to the temperature behavior of $\text{YBa}_2\text{Cu}_3\text{O}_7$). The difference in the temperature dependence between S_p and S_c in $\text{YBa}_2\text{Cu}_3\text{O}_7$ is consistent with the difference of temperature dependence between ρ_c and ρ_p . The temperature dependence of S_c is similar to that of S_p in agreement with the temperature dependence of ρ_c and ρ_p . Together with the Hall effect,^{1,21-23} the unusual transport properties in the high- T_c superconductors may be related to the unconventional electronic structure of highly correlated electrons in the high- T_c superconductors.

Because of the highly anisotropic electronic structure of high- T_c superconductors and their unusually high critical temperatures, the dimensionality of the superconductivity is one of the major interests in mechanistic studies. In the $\text{YBa}_2\text{Cu}_3\text{O}_7$ system, three-dimensional superconductivity theory was reported to fit some of the experimental results, while two-dimensional theory fits other results. Furthermore, a crossover from two-dimensionality to three-dimensionality was observed.^{7,8} For the $\text{Bi}_2\text{Sr}_{2.2}\text{Ca}_{0.8}\text{Cu}_2\text{O}_8$ system, two-dimensional superconductivity theory has been deemed applicable in most experiments.⁹ The paraconductivity results on polycrystalline Tl-Ba-Ca-Cu-O bulk samples and thin films can be fit with two-dimensional superconductor theory.^{8,9} The paraconductivity and dimensionality of 2:2:1:2 single crystals will be discussed here.

Above T_c the total conductivity could be enhanced by the unstable Cooper pairs. The strictly linear R versus T curve in the high-temperature region ($> 240 \text{ K}$) may be recognized as a sign of resistance not associated with fluctuation conductivity. We assume that the normal-state resistivity remains linear to the transition. Where the measured resistivity deviates from this behavior we assume that the deviation is due to fluctuation conductivity. In discussions of paraconductivities of high- T_c systems, the Maki-Thompson term from the pair breaking has been regarded as negligible and it has been ignored here.^{8,10,24} The excess conductivity from the superconducting fluctuations are then derived by the subtraction of the normal conductivity from the experimental conductivity. Theoretically, the enhancement of the conductivity can be written as²⁵

$$\Delta\sigma(T) = \frac{e^2}{16\hbar d} (T/T_c - 1)^{-1} \quad (1a)$$

for the two-dimensional (2D) case,

$$\Delta\sigma(T) = \frac{e^2}{32\hbar\xi(0)} (T/T_c - 1)^{-1/2} \quad (1b)$$

for the isotropic three-dimensional case, and

$$\Delta\sigma(T) = \frac{e^2}{16s\hbar} \left[1 + \left[\frac{2\xi_c(0)}{s} \right]^2 (T/T_c - 1)^{-1} \right]^{-1/2} \times (T/T_c - 1)^{-1} \quad (1c)$$

for the intermediate case.²⁶ Here $\Delta\sigma$ is the paraconductivity, $\xi(0)$ is the coherence length at zero temperature, \hbar is Planck's constant, d is the thickness of the 2D superconducting layer, and s is the periodicity of the superconducting layers.

The paraconductivity is often discussed in terms of the $\ln\Delta\sigma$ versus $\ln(T/T_c - 1)$ plot. By choosing the temperature at the middle point of the 10–90 % transition as the transition temperature T_c (104.7 K for sample No. 1 and 99 K for sample No. 2, respectively), we plot $\ln\Delta\sigma$ versus $\ln(T/T_c - 1)$ (Fig. 2). Two-dimensionality is observed in the high-temperature range for all the samples we measured. In some samples, however, a slope change from about -1 , corresponding to two-dimensionality, to about $-\frac{1}{2}$, corresponding to the three-dimensional system, is observed.

The plot shapes and the values of the slopes of $\ln\Delta\sigma$ versus $\ln(T/T_c - 1)$ are very sensitive to the choice of value of T_c , and a poor choice of T_c may cause a wrong conclusion of the dimensionality. The fluctuation conductivity, on the other hand, smears the transition and makes it very difficult to determine the T_c . To avoid the

difficulty in choosing an appropriate T_c , a method *without* adjustable parameters, similar to the one by Kim *et al.*,¹⁰ is therefore used in the following discussion. We rewrite (1a) or (1b) as

$$(\Delta\sigma)^{-1/\alpha} = A^{1/\alpha} (T/T_c - 1), \quad (2)$$

where, for two-dimensional theory, $\alpha=1$ and $A=e^2/16\hbar d$, and for three-dimensional theory, $\alpha=\frac{1}{2}$ and $A=e^2/32\hbar\xi(0)$. Differentiating, we then have

$$\ln \left[-\frac{d(\Delta\sigma)}{dT} \right] = \ln \left[\frac{\alpha A (1/\alpha)}{T_c} \right] + \left[1 + \frac{1}{\alpha} \right] \ln(\Delta\sigma). \quad (3)$$

The parameter α can be deduced from the slope of the plot of the left-hand side of (3) versus $\ln\Delta\sigma$. Figure 3 shows this plot for the data taken on sample No. 1 and sample No. 2 parallel to the a - b plane. The solid and dashed lines correspond to two- and three-dimensional theory, respectively. The paraconductivity in the a - b planes for all the measured crystals may be fit by the two-dimensional theory from 150 K to ~ 2 K above the zero-resistance temperature. For some samples, the crossover from two to three dimensions takes place several degrees above zero-resistance temperature (for sample No. 1, 6 K above zero-resistance temperature of 101 K), and for others, two-dimensional behavior persists to 2.5 K above zero resistance. The crossover may be related to the formation of Josephson junctions between the Cu-O layers. The two-dimensional property in the 105–155 K region is consistent with results from bulk polycrystalline samples and thin films.^{8,9} No crossover

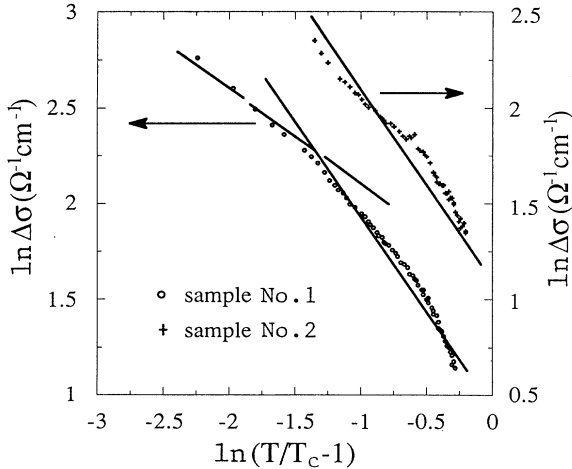


FIG. 2. Plots of $\ln(\Delta\sigma)$ vs $\ln(T/T_c - 1)$. The solid line and dashed line correspond to two-dimensional and three-dimensional superconductivity, respectively. In the high-temperature range, the superconductivity is two dimensional. At low temperature, the superconductivity in some samples becomes three dimensional. The T_c 's used are middle point temperature of 10–90 % superconducting transition.

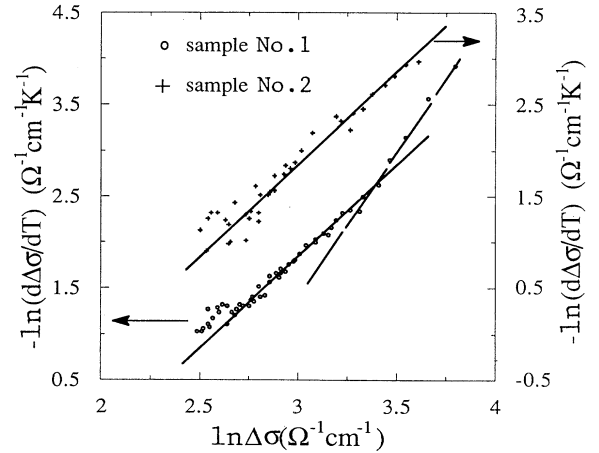


FIG. 3. Plot of $\ln[d(\sim\Delta\sigma)/dT]$ vs $\ln(\Delta\sigma)$. The solid line and dashed line correspond to two-dimensional and three-dimensional superconductivity, respectively. Superconductivity of sample No. 2 is two dimensional. In the high-temperature range, the superconductivity of sample No. 1 is two dimensional, and becomes three-dimensional in the low-temperature range.

was reported in these samples. The lack of crossover may be caused by inhomogeneities in these polycrystalline samples.

The parameter d , the thickness of the superconducting layer, may be estimated to be $\sim 9 \text{ \AA}$ by the intercept in Eq. (3). This value is slightly smaller than the 11.6 \AA spacing between the Cu-O planes. The values estimated here are smaller than the values estimated by a similar measurement on polycrystalline thin films.⁸ The sample-dependent crossover suggests that the attempt to estimate the d parameter should be based on extremely accurate single-crystal data. No attempts to fit the c -axis data to the framework of paraconductivity were undertaken because there is no linearity in the resistance-temperature variation in the normal-state c -axis resistivity data.

CONCLUSIONS

The resistivity of the Tl-based 2:2:1:2 single crystals in the a - b plane is $\sim 4 \times 10^{-4} \Omega \text{ cm}$ and, along the c axis, is

$\sim 0.2 \Omega \text{ cm}$. The temperature dependence of the c -axis conductivity can be explained by a normal metal model with a mean free path comparable with the interplanar spacing of the system near the Mott limit. The electronic bands may be metallic in all directions, but the effective mass is highly anisotropic. The paraconductivity reflects a two-dimensional superconducting nature in these crystal structures. A crossover from two- to three-dimensional behavior as T_c is approached from above is observed in some single crystals.

ACKNOWLEDGMENTS

We would like to thank D. Phillips, G. Parks, and M. Dreiling of Phillips Petroleum for their help with measurements of the single-crystal quality. We also would like to thank B. Dlugosch for his help. This work is supported by Phillips Petroleum company and the Office of Naval Research, Grant No. N00014-90-J-1571.

-
- ¹S. W. Tozer, A. W. Kleinsasser, T. Penney, D. Kaiser, and F. Holtzberg, *Phys. Rev. Lett.* **59**, 1768 (1987).
²S. Hagen, T. W. Jing, Z. Z. Wang, J. Horvath, and N. P. Ong, *Phys. Rev. B* **37**, 7928 (1988).
³S. Martin, T. Fiory, F. M. Fleming, L. F. Schneemeyer, and J. V. Waszczak, *Phys. Rev. Lett.* **60**, 2194 (1988); J. H. Wang, G. Chen, X. Chu, Y. Yan, D. Zheng, Z. Mai, Q. Yang, and Z. Zhao, *Supercond. Sci. Technol.* **1**, 27 (1988).
⁴Y. Iye, T. Tamegai, H. Takeya, and H. Takei, *Jpn. J. Appl. Phys.* **27**, 658 (1988).
⁵H. M. Duan, L. Lu, and D. L. Zhang, *Solid State Commun.* **67**, 809 (1988).
⁶P. P. Freitas, C. C. Tusei, and T. S. Herbert, *Phys. Rev. B* **36**, 833 (1987).
⁷B. Oh, K. Char, A. D. Kent, M. Naito, M. R. Beasley, T. H. Gaballe, R. H. Hammond, and A. Kapitulnik, *Phys. Rev. B* **37**, 7861 (1988).
⁸N. P. Ong, Z. Z. Wang, S. Hagen, T. W. Jing, and J. Hovarth, *Physica C* **153-155**, 1072 (1988).
⁹A. Poddar, P. Mandal, A. N. Das, B. Ghosh, and P. Choudhury, *Physica C* **159**, 231 (1989).
¹⁰D. H. Kim, A. M. Goldman, J. H. Kang, K. E. Gray, and R. T. Kampwirth, *Phys. Rev. B* **39**, 12 275 (1989).
¹¹H. C. Montgomery, *J. Appl. Phys.* **42**, 2971 (1971).
¹²B. F. Logan, S. O. Rice, and R. F. Wick, *J. Appl. Phys.* **42**, 2975 (1971).
¹³F. Zuo, M. B. Salamon, T. Datta, K. Ghiron, H. M. Duan, C. Dong, W. Kiehl, and A. M. Hermann (unpublished).
¹⁴Lin Shu-yuan, Lu Li, Zhang Dian-lin, H. M. Duan, and A. M. Hermann, *Europhys. Lett.* **12**, 641 (1990).
¹⁵P. W. Anderson and Z. Zou, *Phys. Rev. Lett.* **60**, 132 (1988).
¹⁶V. A. Marchenko, *Fiz. Tverd. Tela (Leningrad)* **15**, 1893 (1973) [*Sov. Phys. Solid State* **15**, 1261 (1973)].
¹⁷Z. Fisk and G. W. Webb, *Phys. Rev. Lett.* **36**, 1084 (1976).
¹⁸M. Gurvitch and A. T. Fiory, *Phys. Rev. Lett.* **59**, 1337 (1987).
¹⁹Z. Z. Wang and N. P. Ong, *Phys. Rev. B* **38**, 7160 (1988).
²⁰Lu Li, Ma Bei-hai, Lin Shu-yuan, Duan Hong-min, and Zhang Dian-lin, *Europhys. Lett.* **7**, 555 (1988).
²¹Hong-min Duan, Lu Li, Wang Xie-mei, Lin Shu-yuan, and Zhang Dian-lin, *Solid State Commun.* **64**, 489 (1987).
²²Y. Lu, Y. F. Yan, H. M. Duan, L. Lu, and L. Li, *Phys. Rev. B* **39**, 729 (1989).
²³J. Clayhold, N. P. Ong, P. H. Hor, and P. W. Chu, *Phys. Rev. B* **38**, 7016 (1988).
²⁴T. Lambezger and L. Coffey, *Phys. Rev. B* **38**, 7508 (1988).
²⁵L. G. Aslamazov and A. I. Larkin, *Fiz. Tverd. Tela (Leningrad)* **10**, 1104 (1968) [*Sov. Phys. Solid State* **10**, 875 (1968)].
²⁶W. E. Lawrence and S. Doniach, *Proceedings of the 12th International Conference of Low Temperature Physics, Kyoto, 1970*, edited by Eizo Karda (Keigaku, Tokyo, 1971), p. 361.